CHAPTER 7:

DEPOSITION OF SILVER ON THYMINE MODIFIED AU(111)

In chapter 6 of the thesis, we have presented that the copper underpotential deposition (UPD) on the Au(111) electrode is strongly supported by the physisorbed thymine molecules. This unexpected behaviour originates from the difference between adsorption energies of thymine on the bare Au(111) electrode and the copper adtoms. It is evident that this energy gain vanishes if one tries to deposit copper ions on a thymine modified copper substrate.

Thymine molecules do not only physisorb on the Au(111) electrode in a flat orientation, but also chemisorb in an upright orientation at positive potentials. In the present chapter, we investigated how the Au(111) electrode, modified by perpendicular oriented thymine molecules, behaves in terms of metal deposition processes. To answer this question, the silver underpotential as well as overpotential deposition on the Au(111) electrode, which is modified by chemisorbed thymine molecules, have been examined by electrochemical experiments combined with photoemission experiments.

Firstly, a brief introduction into the problems of Ag UPD on the Au(111) electrode in pure perchlorate solution is given. Secondly the influence of the chemisorbed thymine on the UPD/OPD of silver is presented and discussed.

7.1 Silver deposition on Au(111) electrode

The underpotential deposition of silver on the Au(111) electrode in different electrolytes has been studied using electrochemical [165-167], spectroscopic [168], AFM [50], STM [165, 166, 169, 170], SEXAFS [171, 172], EQCM [173] and SHG [174] techniques. Although, the UPD of silver on Au(111) in different electrolytes has been studied by numerous authors, there are still discrepancies

between the results of different groups, mainly related to the adsorbate structure and to the coulometry in sulfuric and perchloric acid solutions.

According to the studies of Itaya [166], Esplandiu [170] and Garcia [165], the voltammetric profile for Ag UPD on Au(111) electrodes both in perchloric and sulfuric acid media shows three well-defined pairs of peaks at approximately the same potentials (0.4 V, 0.0 V, -0.1 V vs. Ag/Ag^{+}). Peaks in sulfuric acid media, especially those at the most positive potentials, are sharper than those in perchloric acid. The STM studies revealed that in perchloric acid solution only a (4 x 4) structure is formed, whereas in sulphuric acid solution a $(\sqrt{3} \times \sqrt{3})R30^{o}$ structure was found in the region between the first and second peaks [165, 166]. No well-resolved atomic-scale image was observed for the second UPD peak. After the third UPD peak, a (1 x 1) commensurate structure is observed by STM both in perchloric and sulfuric acid media [165, 166, 169, 170]. Itaya and co-workers calculated the charge involved in the entire UPD process as 270-285 μCcm^{-2} [166] whereas Esplandiu and co-workers found it as 380 μCcm^{-2} [170] in sulphuric acid solution. The charge required for the deposition of a (1 x 1) layer of silver (assuming $Ag^{+} + e^{-} \longrightarrow Ag$) would be 222 μCcm^{-2}. Since the measured charge also has contributions due to the adsorption/desorption of anions, it would be expected that some anions desorb upon silver deposition. EQCM [173] measurements have indeed shown that anions are desorbed during the first UPD peak, probably giving rise to the excess charge found in the coulometry. Electron spectroscopies including AES and CEELS confirm that significant quantities of anions are incorporated into the Ag lattice [175]. In perchloric acid, the Ag-Ag distance in the adlayer measured by SEXAFS [171, 172] is 2.88 $\pm$ 0.03 Å, which is almost the same as the Au-Au distance. SEXAFS studies suggested the existence of additional oxygen atoms on the adlayer [172] probably from adsorbed water or perchlorate. These studies also revealed that silver, unlike copper, is fully reduced and occupies the 3-fold hollow sites [171]. The 3-fold geometry is also suggested by SHG [174].

In our study, we have examined the deposition of Ag in pure perchloric acid solution using cyclic voltammetry, chronocoulometry, EC-STM and XPS techniques. Ag UPD on Au(111) occurs within a potential range where a surface reconstruction of the substrate can be excluded. Fig. 7.1 represents the cyclic voltammograms obtained at 20 mV/s (a) and 2 mV/s (b) scan rates

for the UPD of Ag on Au(111) in 1 mM $AgClO_4$, 0.100 M $HClO_4$ and 0.060 M $NaClO_4$ showing two minor ($C_{1,2}/A_{1,2}$) as well as one major (C_3/A_3) peak pairs.

These results are not in good agreement with the published data at which a relatively sharp peak pair were observed at positive potentials [166]. According to Gewirth and co-workers [50] the variation in voltammetry in perchlorate may reflect greater sensitivity of this system to surface structure or to small amounts of contaminants. Besides, perchlorate anion is not strongly specifically adsorbed as much as most of other studied electrolytes (SO_4^{2-}, halides). The lack of specific adsorption may make the voltammetry in the perchlorate system more sensitive for adsorbing impurities.

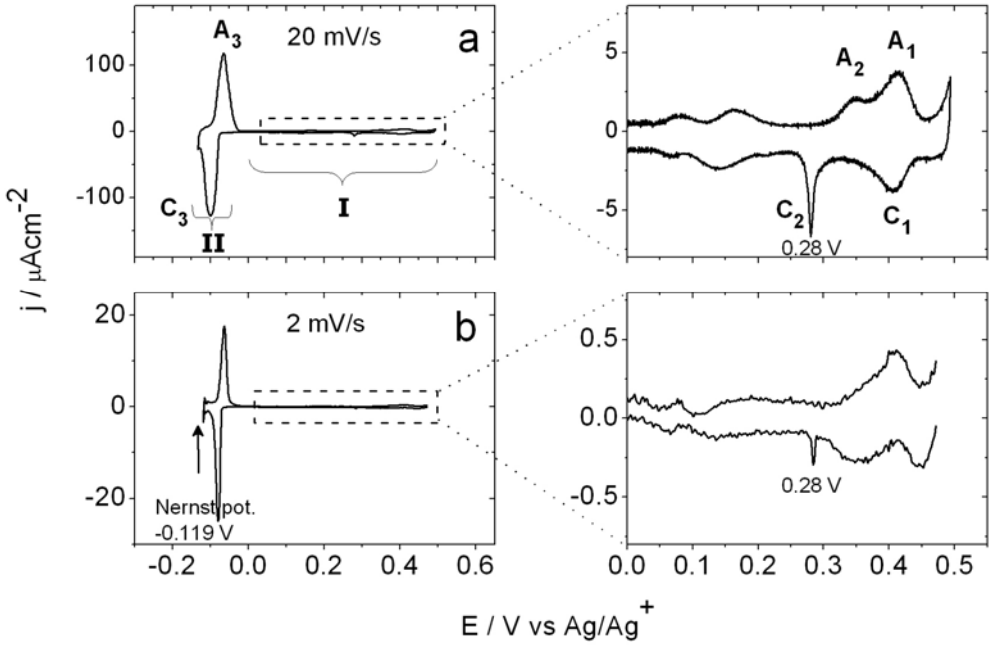

Figure 7.1: *Cyclic voltammograms of Au(111) in 1 mM $AgClO_4$, 0.1 M $HClO_4$ and 0.06 M $NaClO_4$ at scan rates of 20 mV/s (a) and 2 mV (b) (zoomed regions are at right side).*

Roughly, the voltammograms shown in Fig. 7.1 can be divided into two potential regions, *(I)* and *(II)*. In *region I*, only small current waves indicate the presence of already adsorbed silver adatoms at the surface. The needle peak (C_2) at 0.28 V, which does not depend on scan rate, is seen only at fresh flame annealed surfaces and depends therefore strongly on the quality of the Au(111) surface. The broad anodic peak (A_2) might be the stripping of the needle signal, C_2. The main deposition (charge transfer) takes place in the potential *region II*. The charge values

calculated from the integration of cathodic sweep (without double layer correction) in the *region I* and *II* are about 60 ± 15 μCcm^{-2} and 202 ± 10 μCcm^{-2}, respectively.

7.1.1 Chronocoulometric Studies

In order to be sure about the charge and the deposition-dissolution mechanisms of Ag UPD, we have performed chronocoulometric experiments according to three different sets of routines.

Formation transients

In this set, we obtained the formation transients based on the following routine: The Au(111) electrode was immersed at 0.5 V into the solution containing 1 mM $AgClO_4$ under potential control (supporting electrolyte: 0.060 M $NaClO_4$, 0.100 M $HClO_4$). A potential jump into the negative potentials was applied and the current-time curves were recorded. Two representative formation transients recorded at the formation potentials at 0.000 V and -0.085 V are shown in Fig. 7.2.

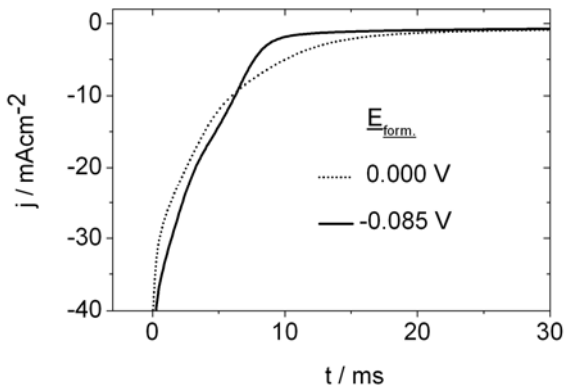

Figure 7.2: *The formation transients measured at three different formation potentials.*

The typical minimum/maximum transient indicating a nucleation and growth process was not observed. It was found formerly for the copper underpotential deposition (section 5.3.2). Besides, the adsorption process is very fast because most of the deposition is completed at the very beginning of process.

7.1.1.a Dissolution transients I

In this set of routines, we have used two different formation potentials; 0.000 V and -0.085 V corresponding to the potential *region I* and *II*, respectively. In region II, we adjusted the electrode at the peak position, which is 30-35 mV positive of the Nernst potential of Ag, to avoid the bulk deposition. Using the following sequence of potential sweep and step routines, the current transients were obtained (Fig. 7.3) in the electrolyte containing 1 mM $AgClO_4$ (supporting electrolyte: 0.060 M $NaClO_4$, 0.100 M $HClO_4$).

(1) Scanning from 0.5 V (at which less or no silver ions are adsorbed on the gold surface) to the formation potentials (-0.085 V and 0.000 V) with a scan rate of 5 mV/s,

(2) Waiting at the formation potentials for different times,

(3) Stepping from the formation potentials to 0.5 V where no deposition occurs and parallel to that the dissolution transients were recorded.

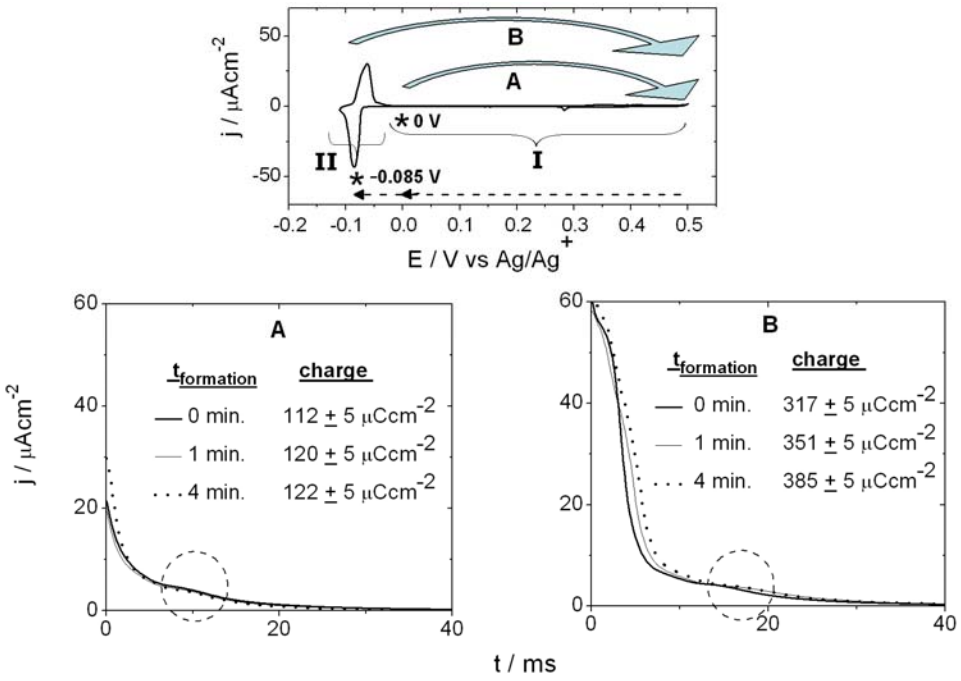

Figure 7.3: *The cyclic voltammogram on which the coulometric measurements are based in the electrolyte of 1 mM $AgClO_4$, 0.100 M $HClO_4$ and 0.060 M $NaClO_4$ with the sweep rate of 5 mV/s. The arrows show the routines of the potential-step experiments. (A,B) Dissolution transients obtained after waiting different times at formation potentials (0.000 V, -0.085 V for A and B, respectively) and stepping into the dissolution potential 0.500 V.*

The transients, A, B, shown in Fig. 7.3 do not have well-defined minimum-maximum peaks as observed in the copper system. However, in the transient series of A and B, the small shoulders around 10 ms might be a sign for the overlap of nucleation and growth mechanism with some other kinds including surface diffusion controlled one during the dissolution of the first ML of Ag.

The charge values calculated by integration of the dissolution transients are associated with the charge consumption during the deposition process. However, the change of PZC has to be considered due to that PZC of Ag(111) differs by -1 V [176] compared to the PZC of Au(111). It is generally assumed that the PZC of a bare surface shifts to negative values during UPD and becomes the PZC of the second metal after formation of a monolayer [170]. During the change of PZC (monolayer formation), the amount of the anodic charge $\int_{PZC}^{PZC'} C_{DL}\,dE$ is 50 ± 5 μCcm^{-2}, where C_{DL} is the double layer capacitance calculated from the capacitive curve of 1 mM Ag^+ electrolyte (Fig. 7.4). If we assume the completion of monolayer of Ag around -0.060 V, a significant change is observed at PZC. This change might influence the measured charge values remarkably. Besides the effects caused by the change of PZC, capacitive contribution and anion adsorption also makes our calculation more complicated. However, we neglected it during our calculations.

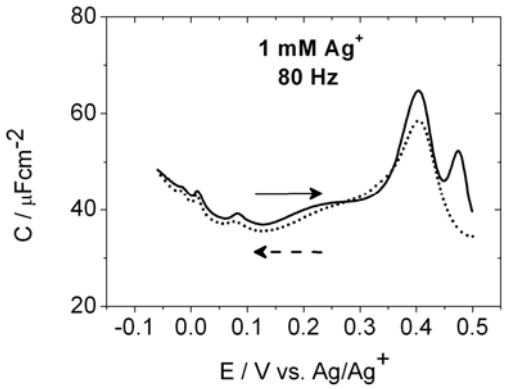

Figure 7.4: *The capacity-potential curve of 1 mM $AgClO_4$, 0.100 M $HClO_4$ and 0.060 M $NaClO_4$. Perturbation frequency: 80 Hz. Amplitude: 3 mV.*

The integration of the dissolution transients (Fig. 7.3) gives the charge values as shown together with the transients. We can summarize the results as follows:

i) The formation of the first silver monolayer is almost finished after attaining the formation potential of 0 V. The consumed charge increases slightly upon waiting there to the value of 122 $\pm$ 5 μCcm^{-2}.

ii) Contrarily, the charge consumed during the formation of the second silver monolayer increases by about 20 % within 4 minutes. This reveals that this process is accompanied by a long time ordering process. The total charge consumed during the whole UPD range is about 385 $\pm$ 5 μCcm^{-2}.

7.1.1.b Dissolution transients II

The following routine was performed in this set:

(1) Scanning from 0.5 V to different final potentials (E_f) at the scan rate of 5 mV/s.

(2) Without waiting at E_f, a potential step to beginning potential, 0.5 V and the dissolution transients were recorded.

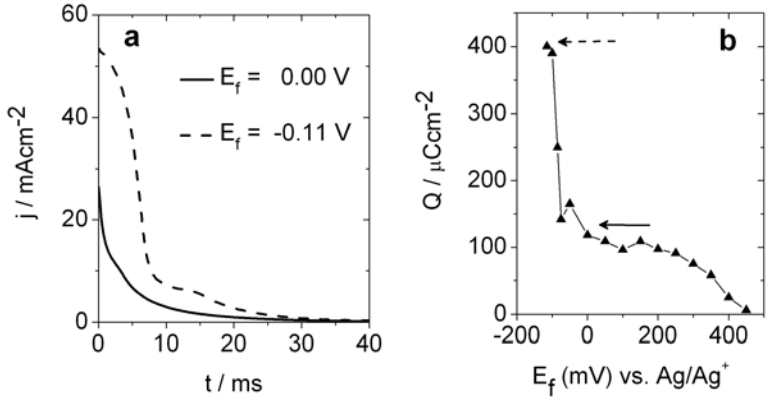

Figure 7.5: *Two representative dissolution transients (a) recorded according to the procedure above and the charge density-potential diagram (b) integrating the transients.*

Two corresponding dissolution transients for the final potentials, E_f, are shown in Fig. 7.5.a. The solid curve, which exponentially decays, represents the dissolution transient at the final potential of 0.00 V. It implies that the adlayer possesses one type of structure. However, the dashed curve representing the transient at the final potential of -0.110 V is formed by the following two consecutive parts; the dissolution of the second monolayer at the beginning (0-10 ms) and the dissolution of the first monolayer (10-30 ms).

The integration of the dissolution transients recorded at different final potential gives the charge density-potential curve as shown in Fig. 7.5.b. The consumed charge density during the dissolution of the first monolayer (formed at -0.060 V) is about 140 $\pm$ 10 μCcm^{-2}, which corresponds to 0.6 $\pm$ 0.05 ML of fully discharged silver adatoms. This value is smaller than the comparable values reported for silver deposition in sulphuric acid electrolyte (0.70 $\pm$ 0.05 ML [170], 0.88 $\pm$ 0.05 ML [177], 0.94 $\pm$ 0.07 ML [167, 168].

The charge consumption within the whole UPD region is about 400 $\pm$ 10 μCcm^{-2} indicating the formation of ca. 2 ML of silver. Similar result in sulphuric acid solution has also been reported in the literature [167, 170].

7.1.2 Influence of waiting or cycling within the UPD region

It is interesting that some changes in the voltammograms of Ag UPD have been observed upon waiting or cyclic within the UPD region. These changes upon waiting at 0.00 V (a) and repetitive cycling (b) in CVs are shown in Fig. 7.6. The appearance of a new small reversible peak at 0.48 V starts after waiting half an hour at 0.00 V or cycling 10 times (~ 30 minutes). The main peak pair around -0.1 V, which corresponds to the formation of the second monolayer, decrease considerably with cycling. Similar behaviour of Ag UPD in sulphuric acid solution upon cycling have been observed and reported in the literature [167, 178]. Some authors [167] assigned the peak pair at 0.48 V to a surface disordering process associated with the formation of an Ag-Au alloy. In contrast to some authors [52, 167, 178] observing some changes in voltammograms with cycling, Corcoran et. al. [169] reports no significant change with cycling for a period a few hours in the perchloric acid solutions of silver and claims the absence of alloy formation. However, the reported CV (1st cycle) by Corcoran has the sharp reversible peaks, which indicate that their electrode already covered with chloride adsorbed on the gold surface. In a recent study, Michalitsch et. al. interpret the changes upon cycling on the basis of XPS data as the formation of more noble underpotentially deposited silver layer on gold by the adsorption of chloride [52].

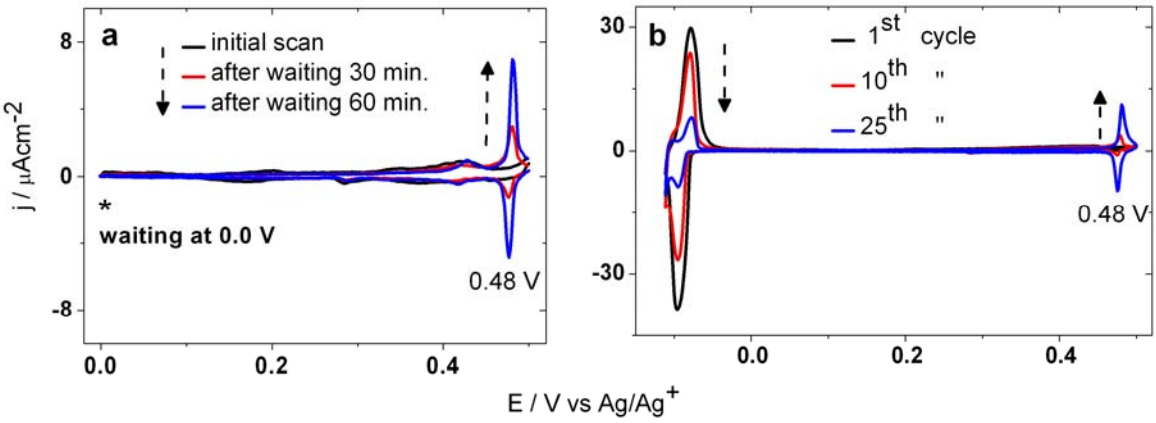

Figure 7.6: *Cyclic voltammograms of Au(111) in 1 mM $AgClO_4$, 0.1 M $HClO_4$ and 0.06 M $NaClO_4$ at the scan rate of 5 mV/s. (a): waited consecutively half an hour at 0.00 V. (b): cycled different times in the UPD region.*

In order to clarify the changes observed upon cycling or waiting in the UPD of silver, we have investigated the behaviour of the adjusted silver layer in the pure perchloric acid solution (0.1 M). Firstly, the electrode was cycled 25 times in silver solution repetitively, and then we removed it at 0.5 V under potential control and afterwards transferred to the perchloric acid solution. It is clearly seen in the voltammograms shown in Fig. 7.7 that the silver species are not removed from the gold surface at once. At each repetitive cycle the stripping peak is always larger than the deposition peak and they vanish as cycling within the UPD region of silver. Interestingly, this peak pair is not as sharp as that observed in Ag^+ solution and locates at relatively negative potentials (ca. 0.35 V).

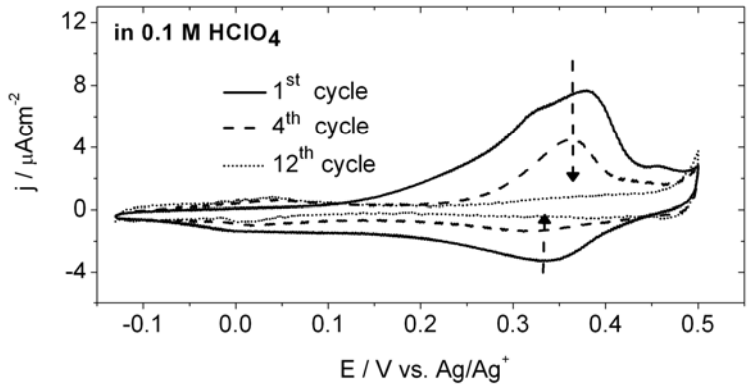

Figure 7.7: *The cyclic voltammograms of Au(111) in 0.1 M $HClO_4$ at the scan rate of 20 mV/s after transferring the cycled electrode in silver solution.*

7.1.3 XPS studies

In order to investigate the binding states of the silver adatoms deposited at different potentials and under different experimental conditions, XPS experiments were carried out with synchrotron radiation (excitation energy 630 eV) at BESSY GmbH.

The transfer procedure was applied as described in the experimental section 3.3.4. This procedure allowed measuring the absolute work function due to the absence of double layer potentials during the transfer.

The spectra in Fig. 7.8 display the differences in binding energies of the 3d electron level of silver adatoms depending on the emersion potential. It can be recognized that no difference at the signal positions exist between the bulk silver (green) and the second monolayer of silver (red) deposited on Au (111) samples. In contrast, the signal arising from the first monolayer (blue) shifts about 260 meV to lower binding energies. The calculation of the areas under the peaks gives reasonable results. The area under the red curve belonging to the 2nd UPD (2A) is almost twice that of 1st UPD (A, blue). Besides, the area under the green curve belonging to the OPD (2.8A) is more than that of the 2nd UPD.

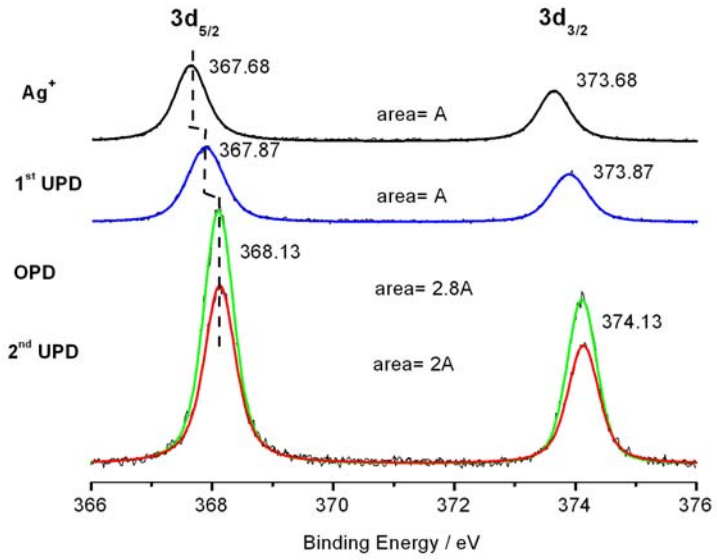

Figure 7.8: *Ag-3d core level spectra of the silver deposited Au(111) electrode at different emersion potentials; 0.530 V (black, after cycling 30 min. in UPD range), 0.00 V (blue), -0.125 V (green), -0.090 V (red).*

The changes in the cyclic voltammograms upon waiting or cycling in the UPD region of silver may be compared with the results of the XPS measurements. The 3d core level signal of silver at the cycled sample (black) downshifts about 450 meV compared to that of the bulk silver (green). This shift coincides with the expected shift occurring in silver salts. Only after long time cycling, one gets evidence in the CV for the presence of chloride ions at the surface (Fig 7.6). Surface coverage of AgCl was calculated giving not more than 0.25 ML with respect to the gold underground after 25 potential cycles. The Cl-2p core level signal obtained from the cycled probe is shown in Fig. 7.9 indicating the AgCl adsorption at the surface. Considering the sensitivity factors of Ag-3d (5.2) and of Cl-2p (0.73), the calculation of the relative intensities of the species gives almost the unity. It supports the idea of formation of AgCl salt at the gold surface, too.

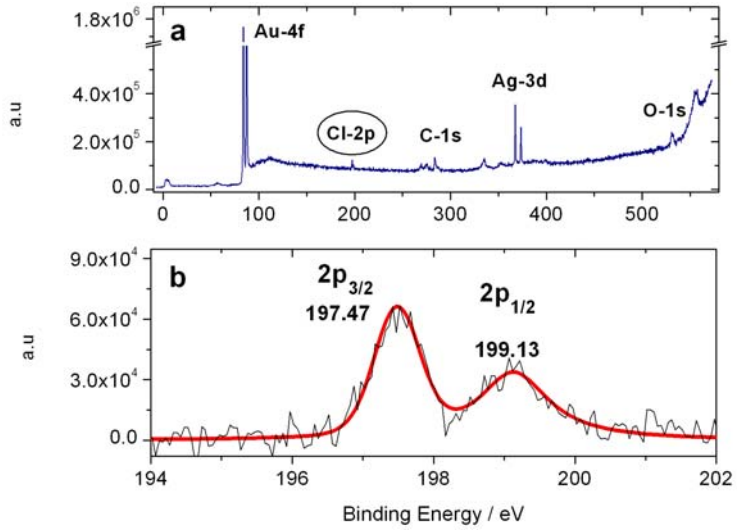

Figure 7.9: *The Cl-2p core level spectrum detected after 25 cycling in silver perchlorate solution emersed at 0.53 V.*

The deviations between our experiments and the findings discussed by Michalitsch et. al.[52] may be due to the differences in the emersion potentials. It should be noticed that both silver species, the reduced and the oxidized forms, interact with chloride ions at positive potentials. Summarizing, we agree well with Michalitsch and coworkers that the sharp needle peak pair around 0.5 V exhibits the oxidation/reduction of silver ions which strongly interact with chloride ions. The possibility of the formation of an Au/Ag surface alloy would cause a 3d band shift to higher binding energies in comparison to the pure form. In none of our experiments we could find any hint on such shift.

In our experiments, the contact between electrolyte and electrode was adjusted not longer than 15 minutes to guarantee of the absence of any interaction between chloride ions and silver adatoms at the gold surface.

7.1.3.a Determination of Work Function

The absolute value of the work function of the different surfaces was identified by measuring the electron cut off by UPS (Fig. 7.10). To determine the work functions, the secondary electron cut off was recorded with the sample biased at -10 eV to clear the analyzer work function. We used the following formula to calculate the work function values of samples;

$$\Phi = h\nu - E_F + E_{cut\,off} - 10$$

The used photons have 35 eV energy. The Fermi energy of the analyzer, E_F, is 30.17 eV. The work functions for a blank Au sample and for the silver first UPD prepared by emersing at 0.000 V were determined within the error range to be 4.9 $\pm$ 0.05 eV. Normally, the work function of gold prepared in UHV etched by argon is around 5.4 $\pm$ 0.05 eV [111]. The lower value for the bare gold surface indicates the presence of some impurities from flame annealing and the transfer. However, for the second monolayer as well as for the bulk silver the close work function values downshift to about 4.67 $\pm$ 0.05 eV.

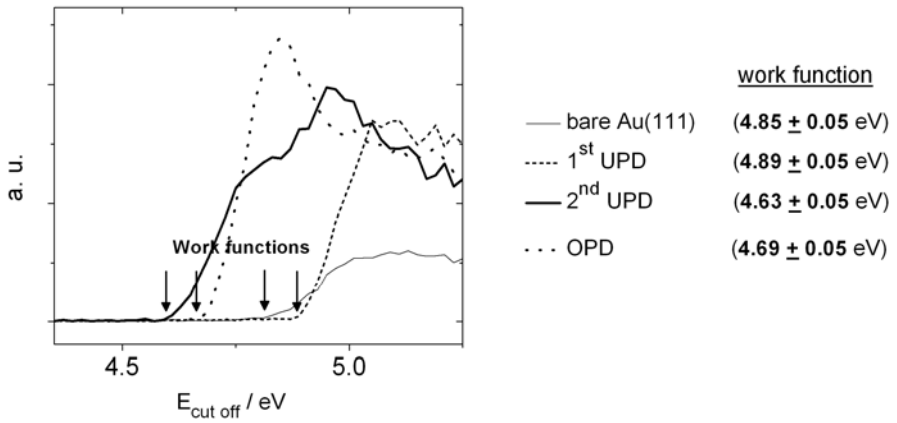

Figure 7.10: *Electron cut off energy measurements to determine the work function values.*

7.1.4 Structures of Ag adlayers

Considering the coulometry and the XPS results, the following adlayer structures formed at 0.000 V (1st region) (a) and at -0.085 V (2nd region) (b) can be proposed (Fig. 7.11). The Ag adlayer formed at higher underpotentials (Fig. 7.11.a) has an expanded (4 x 4) structure as proposed by Ogaki et.al. [166]. We proposed that the oxidation state of silver atoms in this potential region is between 0 and +1 due to that the XPS signal observed in Fig. 7.8 (blue) locates between the signals of metallic and ionic silver species.

At lower underpotentials (~ -0.085 V), almost 2 MLs of metallic silver is formed (Fig. 11.b). We propose an expanded structure for the second ML because the charge value obtained from coulometry does not exactly correspond to full 2 MLs. Besides, the area calculations of the XPS signals shown in Fig. 7.8 also support this idea.

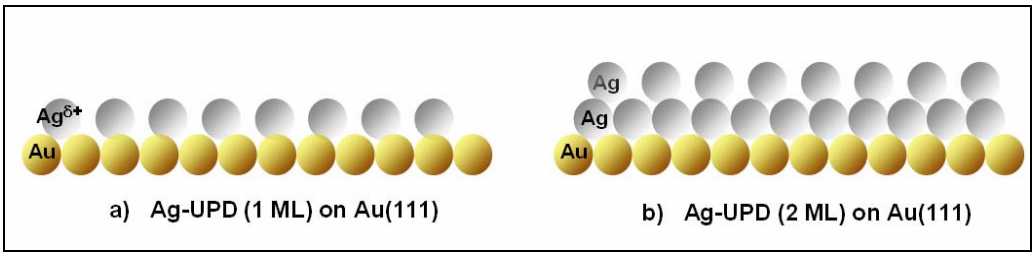

Figure 7.11: *Schematic representations for silver UPD adlayers.*

7.2 Silver deposition on Thymine modified Au(111) electrode

The UPD of silver takes place in potential regions, in which thymine molecules chemisorb on the Au(111) surface [14, 27] (Fig. 7.12). Thymine molecules influence the silver deposition significantly and the main deposition occurs around 0.24 V, which is about 0.3 V positive of the main deposition peak of silver alone. These reversible peaks are broader compared to that in the thymine-free silver solution. One obtains only a negligible shift of the peak positions depending on the thymine concentrations. In the presence of 12 mM thymine in the solution, the formation of the second Ag monolayer is completely suppressed, but the bulk deposition is only slightly inhibited. The strength of the inhibition exhibits a linear dependence to the concentration of thymine in the solution. The oxidation of gold is also inhibited due to the chemisorbed thymine on the Au(111) surfaces.

Almost constant cathodic current density recorded at the negative of deposition peak C_1 (Fig. 7.12.c) gives some hints about the deposition process. With increasing negative potentials, the further silver adatom adsorption behaves like a Langmuir type until a full ML is formed.

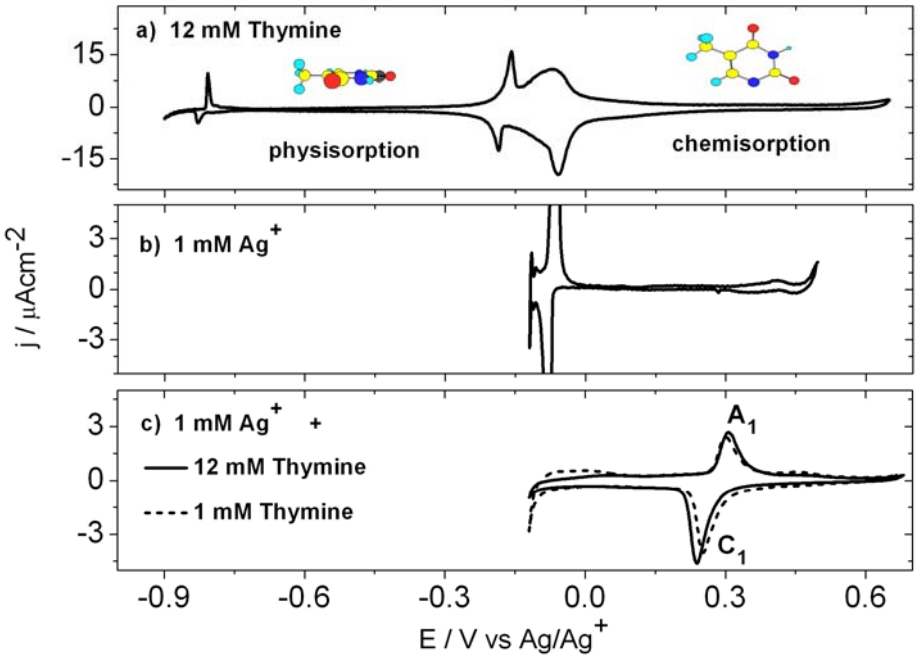

Figure 7.12: *Cyclic voltammograms of Au(111) in* ***a:*** *12 mM Thymine (50 mV/s),* ***b:*** *1 mM $AgClO_4$ (2 mV/s)* ***c:*** *12 mM Thymine + 1 mM $AgClO_4$ (2 mV/s). Supporting electrolyte contains 1 M $HClO_4$ and 0.06 M $NaClO_4$.*

There are two possibilities occurring at the beginning of the deposition of silver in the presence of thymine. These are the coadsorption of silver ions together with thymine molecules and the interaction of silver ions with the chemisorbed thymine molecules on the Au(111). We have examined these possibilities as follows:

Firstly, thymine was adsorbed at the electrode surface at 0.6 V holding 5 minutes in the electrolyte containing 12 mM thymine. Afterwards, the electrode was removed from the electrolyte under potential control and the concentrated Ag^+ solution was added. After purging the solution with argon for further mixing, the modified electrode was immersed again into the electrolyte under potential control at 0.6 V.

The subsequently recorded CV in the Ag UPD range is almost identical to the voltammogram shown in Fig. 7.12.c. This indicates that the silver ions interact with the chemisorbed thymine molecules and penetrate the layer.

7.2.1 Chronocoulometric Studies

The following transients (Fig. 7.13) were obtained using a solution containing 12 mM thymine and 1 mM $AgClO_4$ (supporting electrolyte: 1 mM $HClO_4$ and 0.060 M $NaClO_4$).

The formation transients (a) were obtained jumping from the positive potential of 0.650 V at which almost no silver is deposited into the two different formation potentials of -0.085 V and -0.050 V. We have chosen these formation potentials due to that each one corresponds to one and two monolayer formation in thymine-free silver solutions.

At none of the potentials one could find a typical minimum/maximum transient indicating a nucleation and growth process, which was found formerly for the UPD of copper on thymine modified surfaces. The shapes imply that overlapping of different processes such as silver deposition, thymine desorption or thymine adsorption on top of silver layer can take place.

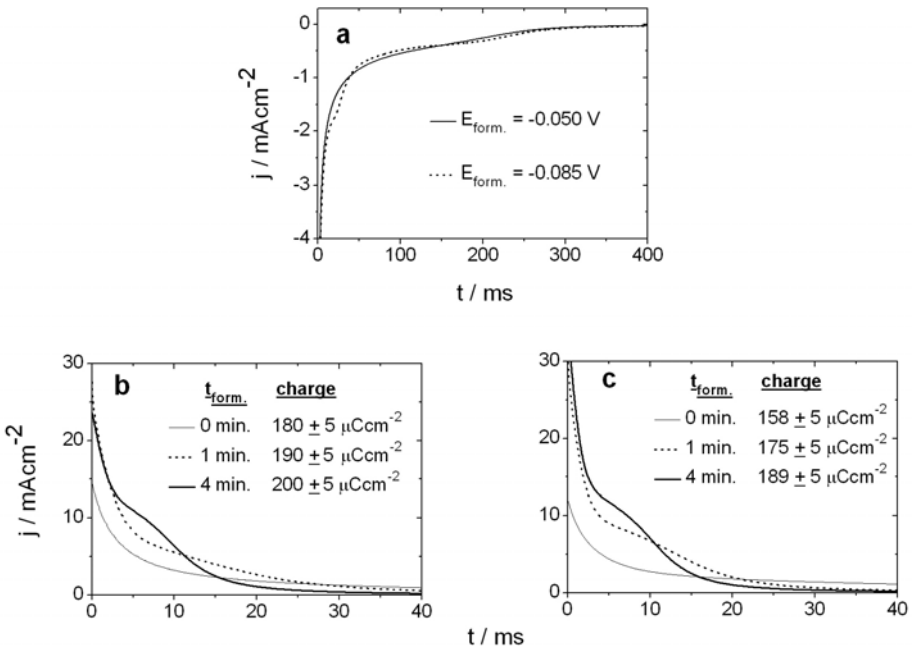

Figure 7.13 a: *The formation transients obtained after jumping from the 0.600 V to the formation potentials of -0.050 V (solid) and -0.085 V (dashed).* ***b,c:*** *The dissolution*

transients and the charge density values obtained after waiting different times at the formation potentials of -0.085 V (b) and -0.050 V (c).

The dissolution transients were obtained scanning from the positive potentials (5 mV/s) up to the formation potentials of -0.085 V (b) and -0.050 V (c). After waiting different times at these potentials, a step into the positive end (0.600 V) was applied and the current density values against time were recorded.

The transients shown in Fig. 7.13.b,c imply that there is no significant differences between (b) and (c), whereas in thymine-free solution both the shapes and the charge values differ remarkably. Obviously, the shapes of transients reveal an overlapping of at least two processes behind the double layer charging. There may be ordered domains of the silver layer in addition to the less ordered ones which dissolve according to different mechanisms and kinetics.

Charge density diagram

The following charge diagram (Fig. 7.15) obtained integrating the dissolution transients at different formation potentials summarize the silver deposition in the presence and the absence of thymine quantitatively. In thymine containing solution, we adjusted the electrode waiting at 0.240 V and 0.180 V, which correspond to the peak position and the stationary region at negative of the peak in the voltammogram (Fig. 7.12.c), respectively.

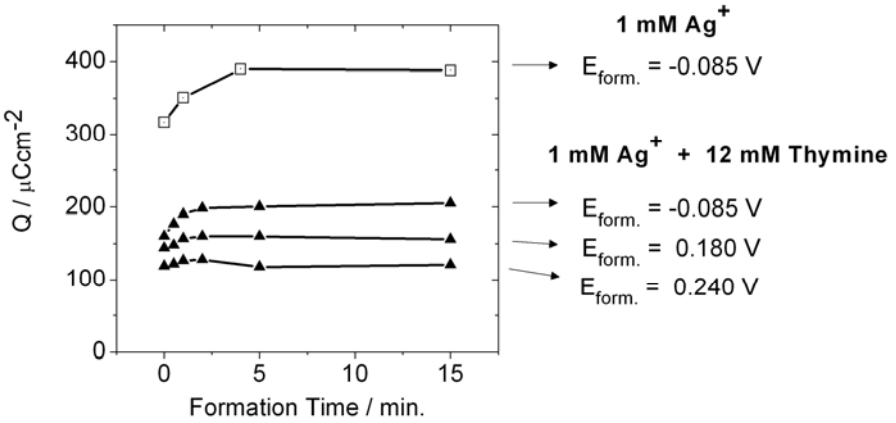

Figure 7.15: *The charge density diagram obtained integrating the dissolution transients in thymine containing silver electrolytes (full triangles) and thymine-free silver electrolyte (open square).*

Independently of the formation potential, it seems that the silver deposition process is mostly finished after about 2 minutes. However the charges consumed during the deposition depends strongly on the formation potential as is the case for deposition on unmodified surfaces. In the presence of thymine, the charge value at – 0.085 V amounts to 200 $\pm$ 5 μCcm^{-2} which is approximately the value for one silver monolayer. Therefore, it can be concluded that only 1 ML is formed in thymine containing silver solution, whereas in thymine-free solution the coverage is close to 2 ML at the same conditions.

7.2.2 Influence of cycling within the UPD region

The repetitive cycling in thymine containing electrolyte exhibits a slightly different behaviour compared to the thymine-free silver solution. The following voltammograms (Fig. 7.16) were obtained cycling 25 times within the UPD range. The small oxidation peaks around 0.48 V (A_1) and 0.00 V (A_3) increase, whereas, the main reversible A_2/C_2 peaks decrease with cycling. In contrast to the thymine-free electrolyte, the observed oxidation peak, A_1, is not reversible. The XPS investigations again showed the chloride species upon cycling. The Cl-2p core level spectrum is identical with that was already observed in thymine-free probes (Fig. 7.9).

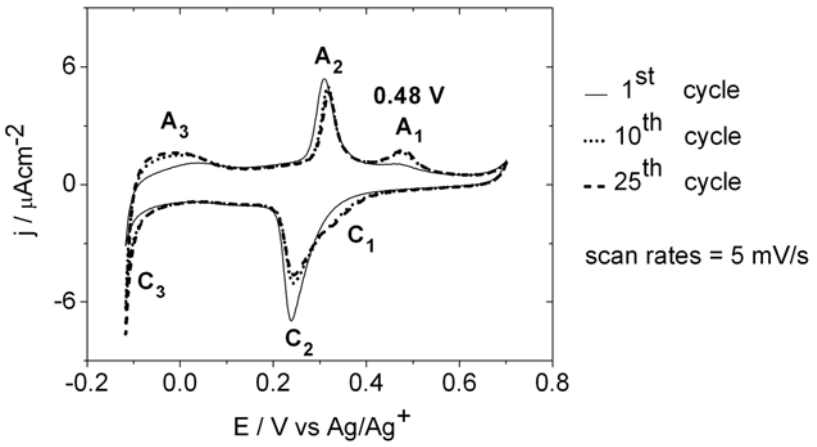

Figure 7.16: *The cyclic voltammograms of Au(111) in 1 mM $AgClO_4$ and 12 mM thymine. The repetitive cycling was applied within the UPD range of silver at 5 mV/s rate.*

7.2.3 XPS Studies

In order to clarify the interaction between thymine and the topmost silver, XPS measurements were carried out using excitation energies of 630 eV. The work function and the core level signals of Ag-3d, C-1s and N-1s were examined.

Work functions

The work functions for thymine/Ag UPD and thymine/Ag OPD systems are higher compared to the thymine-free systems. All work function values are tabulated in Table 7.1.

Au(111)	Au(111) *	
4.85	***5.40***	
Ag 1st UPD	Ag 2nd UPD	Ag OPD
4.89	***4.63***	***4.69***
Thymine + Ag 1st UPD		Thymine + Ag OPD
5.18		***5.38***

Table 7.1: The work function values measured for silver species (± 0.05).

*Argon etched in UHV [111].

Ag-3d

The silver 3d spectra, I and III (Fig. 7.17) were obtained from the solutions containing 12 mM thymine at the emersion potentials of 0.00 V and -0.15 V, where UPD and OPD of Ag take place, respectively. The other two spectra (II, IV) were taken from thymine-free system for comparison.

Spectrum I: Thymine does not make a significant change in the oxidation state of silver compared to the 1st Ag UPD (spectrum II) at which the silver adatoms are partially discharged ($Ag^{\delta+}$).

Spectrum III: Obviously, thymine on the OPD of Ag leads to a downshift (sum curve of III) by 130 ± 10 meV with respect to the 2nd UPD in the thymine-free probe. Since the FWHM of the spectrum III is larger than the others, we divided it to two components. We assume that one component (green, 367.82 eV) corresponds to the third top monolayer of silver at which the silver adatoms are partially discharged like observed in spectra I and II. The other component is at higher binding energy and higher intensity corresponding to 2 ML of metallic Ag.

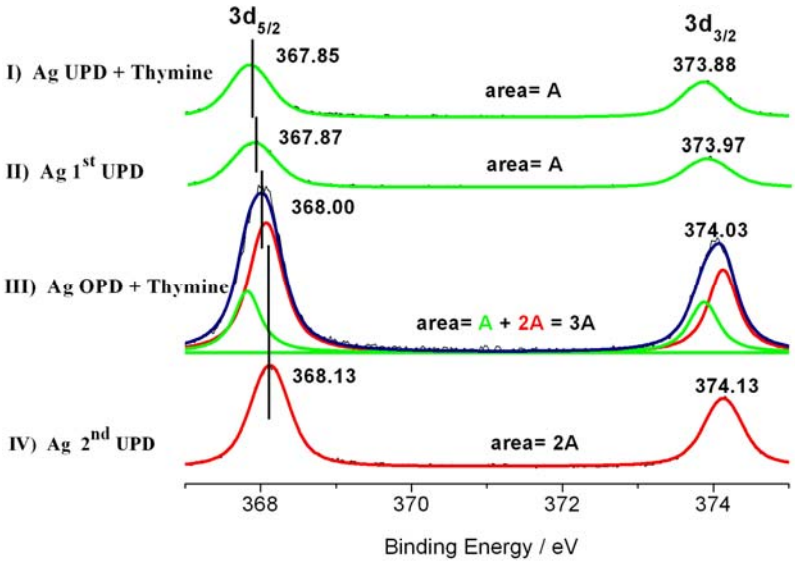

Figure 7.17: *Ag-3d spectra for silver monolayer (I) and bulk silver (III) modified by thymine. The emersion potentials are 0.00 V and -0.15 V for UPD and OPD, respectively. The spectra II and IV are included from thymine-free system for a better comparison.*

C-1s

C-1s signals shown in Fig.7.19 (b,c) reveal that thymine is adsorbed on top of both the UPD and the OPD of silver as similar to the chemisorption on the Au(111) surface (a). These three spectra are not different each other markedly. Four different signals can be distinguished representing different carbon atoms in thymine molecules including the arising at C-C, C-H signals due to the carbon contamination. It can be claimed that carbon atoms do not interact with silver adlayer or gold as the similar spectrum was observed by Kay et. al. [111] in UHV prepared probe.

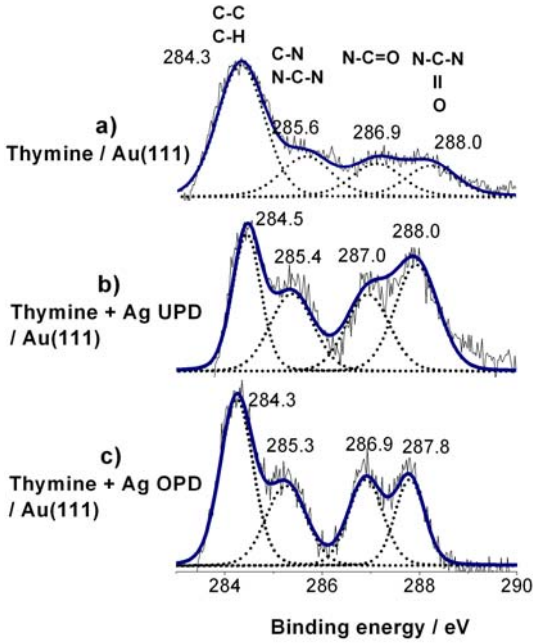

Figure 7.19: *C-1s spectra for the bare Au(111) surface, silver monolayer and bulk silver modified by thymine. The emersion potentials are 0.30 V, 0.00 V and -0.15 V for bare gold, UPD and OPD, respectively.*

N-1s

The existence of an interaction between thymine molecules and the substrate has been observed obviously upon investigating the N-1s signals (Fig. 7.20). Thymine molecules contain two nitrogen atoms N(1) and N(3) (Fig. 6.12). In an early XPS study of thymine, Barber and co-workers determined the energy difference between both nitrogens in a thymine multilayer as 1 eV [53]. However, recently, Kay et. al. measured the difference between the nitrogen signals as about 0.3 eV [111].

We have measured the difference between the binding energies of nitrogens as **1.38** $\pm$ 0.05 eV, **1.60** $\pm$ 0.05 eV and **1.65** $\pm$ 0.05 eV for the chemisorbed thymine on Au(111), thymine on Ag-UPD and Ag-OPD, respectively. In these spectra, the position of the N(1) signal does not change significantly on the different considered substrates. This finding suggest strongly that thymine and the substrate interact via the N(3) nitrogen, which confirms studies about thymine adsorption on Au(111) with SNIFTIRS experiments performed by R. Nichols et. al [14]. The N(3) shift to lower binding energies can be explained by deprotonation leading to an increased electron density due the lone pair at the N(3).

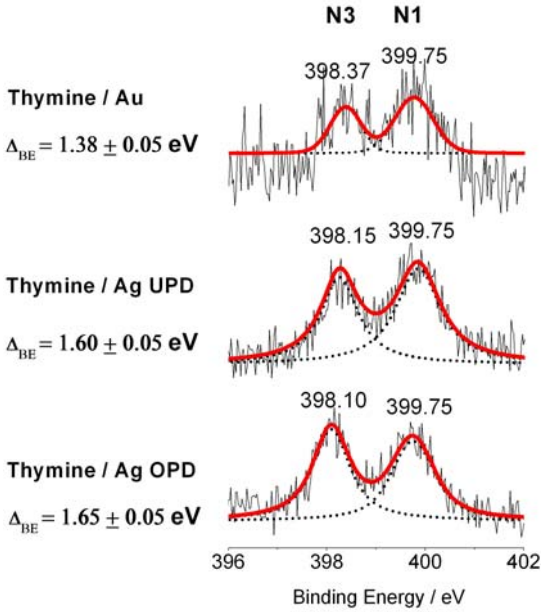

Figure 7.20: *N-1s spectra for the bare Au(111) surface, silver monolayer and bulk silver modified by thymine. The emersion potentials are 0.30 V, 0.00 V and -0.15 V for bare gold, UPD and OPD, respectively.*

The difference between the signals in silver adsorbed species is larger than that of the silver-free one (chemisorbed thymine on Au(111)). That means the electron density on N(3) interacting with silver atoms is higher compared to that interacting with surface gold atoms.

7.2.4 Structures of Ag ML and bulk layer incorporated with thymine

For the structures of UPD and OPD of silver prepared in thymine containing electrolyte, the following representations can be proposed. Negative of the deposition peak (+0.19 V, Fig. 7.12) an expanded silver monolayer is formed as shown in Fig. 7.21. The downshifted Ag-3d signal (Fig. 7.17) reveals that silver atoms are partially discharged in the 1st ML. The following two reasons might be given for partially discharging; one is the monolayer effect and another is the stabilization by deprotonated thymine (electron density on N(3) is high) against fully discharging. In this consideration, partially discharged silver atoms are sandwitched between the deprotonated thymine molecules (via N(3) atom) and gold atoms. Because the partially charged silver adatoms would repel each other, the adlayer has probably an expanded structure even the deprotonated thymine molecules stabilize them.

In bulk potential region (-0.15 V), the topmost silver atoms forming an expanded structure are not fully discharged and interacted with N(3) atom of deprotonated thymine. Whereas, the silver atoms at lower layers have metallic character.

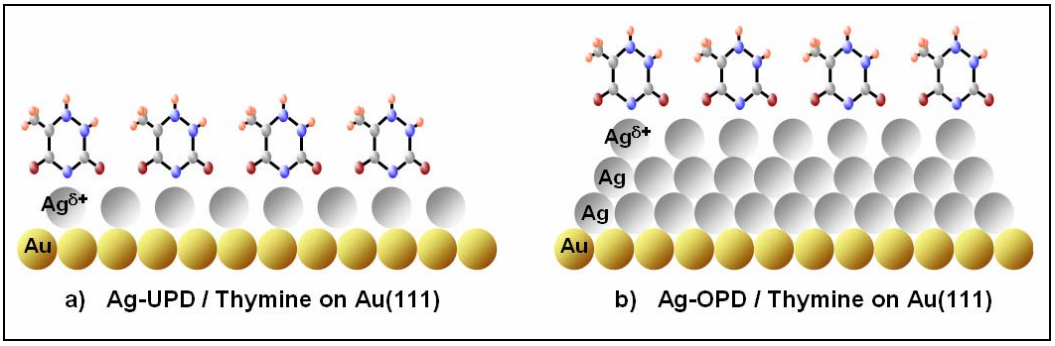

Figure 7.21: *Schematic representations of Cu-UPD (a) and OPD (b) in the presence of thymine.*

7.2.5 STM Imaging of Ag Growth on Au(111)

On the basis of what is already known about the STM and AFM studies presented at the beginning of this chapter, it was our aim to contribute some new findings with respect to the influence of thymine on the deposition process of silver on Au(111). To estimate nucleation and growth behaviour of Ag, Ag deposited Au(111) electrodes were imaged by in situ STM when thymine was absent or present. The measurements were carried out in the potential range of UPD and OPD of silver.

7.2.5.a In the absence of thymine

Figure 7.22 shows consecutive STM images (500 x 500 nm^2) of an Au(111) electrode under various potentials in 1 mM $AgClO_4$ and 0.1 M $HClO_4$. At potentials positive of 0.2 V, STM images exhibit distinctive Au(111) terraces and steps with gold islands which arises from the lifting of the thermally induced surface reconstruction (Fig. 7.22.a). As the potential is moved to -0.050 V, some additional small islands are formed (Fig. 7.22.b). The measurement of the heights of those islands reveals the nucleation and growth of monoatomic and diatomic silver clusters as shown in Fig. 7.22.c. V. Its growth starts at substrate defects such as holes, island rims or step edges. We already know from the chronocoulometric results that almost one monolayer of

silver is formed at -0.050 V within four minutes. However, there is no clear supporting evidence from the STM results for this result.

Upon further scanning to -0.1 V, additional Ag is rapidly deposited and Au(111) terraces and steps disappear entirely but the picture becomes noisy (Fig. 7.22.d). Similar unusual STM image measured in sulphate containing electrolyte was also introduced by Esplandiu and co-workers [170]. The rapid change in the STM picture is a parallel finding with the fast increase in the charge density value measured at the same potential range. Actually, if the experiment was repeated once again at the same potential, we probably would obtain a stationary image having smooth UPD layers as similar to the image of Esplandiu et.al [170]. Summarizing, it is difficult to make a conclusion about the structure of the adlayer at this potential. However, this is not against to the formation of 2 ML of Ag proved by coulometry measurements.

With respect to the overpotential deposition (OPD) of silver on Au(111), a limited *in situ* STM studies have been reported in the literature. Corcoran et al. [51] presented some results obtained by STM in perchloric acid solution, which showed morphological details for the transition from layer-by-layer growth to three-dimensional island growth during electrodeposition. Two epitaxial layers of silver are consecutively formed, followed by heterogeneous nucleation of three-dimensional crystallites, preferentially at steps' edges. These authors proposed that the transition between the two growth modes may be determined by adatom migration over descending steps. Some information about the OPD process in perchlorate solution was also provided by Ogaki and Itaya [166], who found that thick Ag films first show a rolling-hill structure, but become smoother with time owing to surface diffusion.

Our STM images (Fig. 7.22.e-g) obtained in perchloric acid solution at -0.150 V (OPD) are in good agreement with the investigations of Itaya [166] and Esplandiu [170] (in sulphuric acid solution). During waiting at -0.150 V, we observed a perfect layer-by-layer growth (Frank-van der Merwe) rather than a three dimensional growth (Stranski-Krastanov). In contrast to Esplandiu's finding, we have not observed an adlayer (UPD or OPD) topography which is the reproduced of the Au(111) surface.

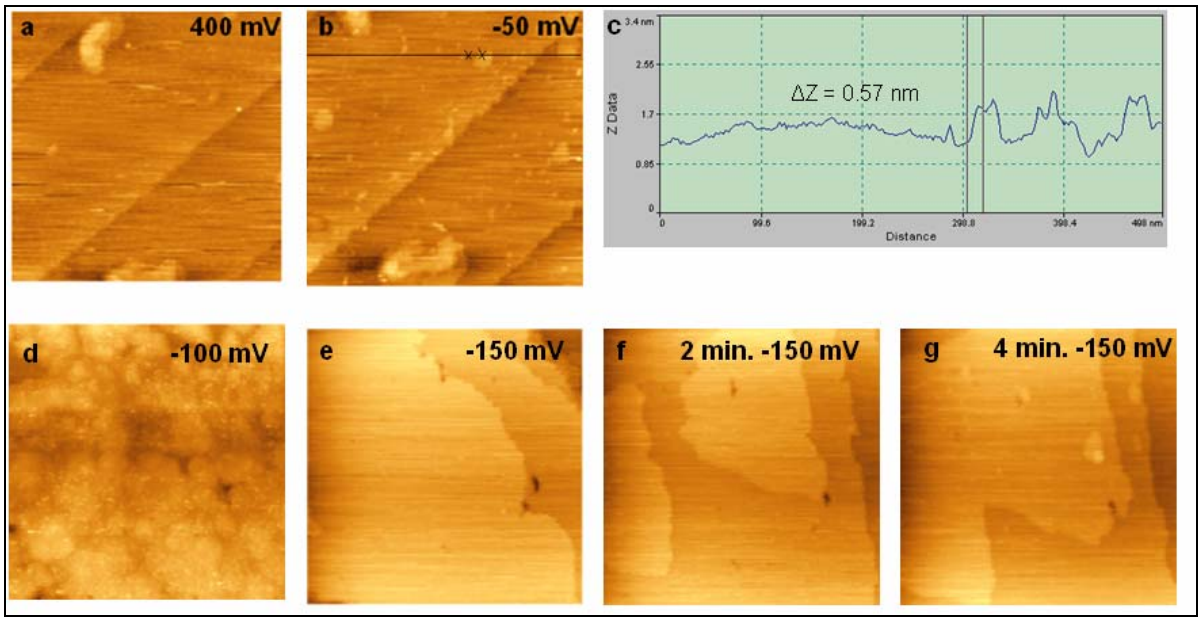

Figure 7.22: *In situ STM images (500 x 500 nm^2) of Au(111) in 1 mM $AgClO_4$ + 0.1 M $HClO_4$, showing the UPD (a, b, d) and the OPD (e-g) processes. I_T = 1 nA, U_{bias} = -0.050 V. All potentials are refer to Ag/Ag^+ (0.1 M).*

7.2.5.b In the presence of thymine

A sequence of *in situ* STM images (500 x 500nm^2) showing the nucleation and growth of Ag in the presence of thymine is presented in Fig. 7.23. The electrolyte contains 12 mM thymine in addition to 1 mM $AgClO_4$ and 0.1 M $HClO_4$.

Considering the cyclic voltammogram of electrolyte described above (Fig. 7.12.c), we obtained the STM images at the potentials; a) 0.350 V: positive of the main peak (C_1/A_1), b) 0.100 V: just negative of the peak, c) -0.080 V: almost end of the UPD, d,e) -0.150 V: OPD.

At positive potentials (E>0.3 V) in silver-thymine solutions, almost no silver is deposited as well as thymine molecules are chemisorbed and upright oriented. The STM image (Fig. 7.23.a) taken at 0.350 V has very large terraces and the density of the gold islands induced by the lifting of reconstruction is very low compared to the thymine-free one (Fig. 7.22.a). The reason of the low density of gold islands is the chemisorption of thymine. Like anions, chemisorbed thymine molecules cause to lift the gold surface islands.

Just negative of the silver deposition peak (0.100 V), the image (Fig. 7.23.b) does not reflect a significant difference compared to the former image. It means that it is difficult to

observe an obvious nucleation and growth mechanism at the first stages of the UPD process. As the potential shift to -0.080 V, formation of some small islands (Fig. 7.23.c) is clearly observed. The heights of those islands vary between 0.15 nm and 0.25 nm (Fig. 7.23.d).

As the potential is moved to -0.150 V (OPD) as well as waiting 2 minutes, Ag islands begin to grow laterally (Fig. 7.23.e,f). Similar to the previous work, a layer-by-layer growth (Frank-van der Merwe) takes place rather than a three dimensional growth (Stranski-Krastanov). The heights of the islands changes between 0.70 nm and 0.90 nm corresponding to sum of the diameter of three Ag atom or one Ag atom and a thymine molecule on top of silver atom. As different from the pure Ag system, the number of nucleation centres is greater in the thymine-Ag system.

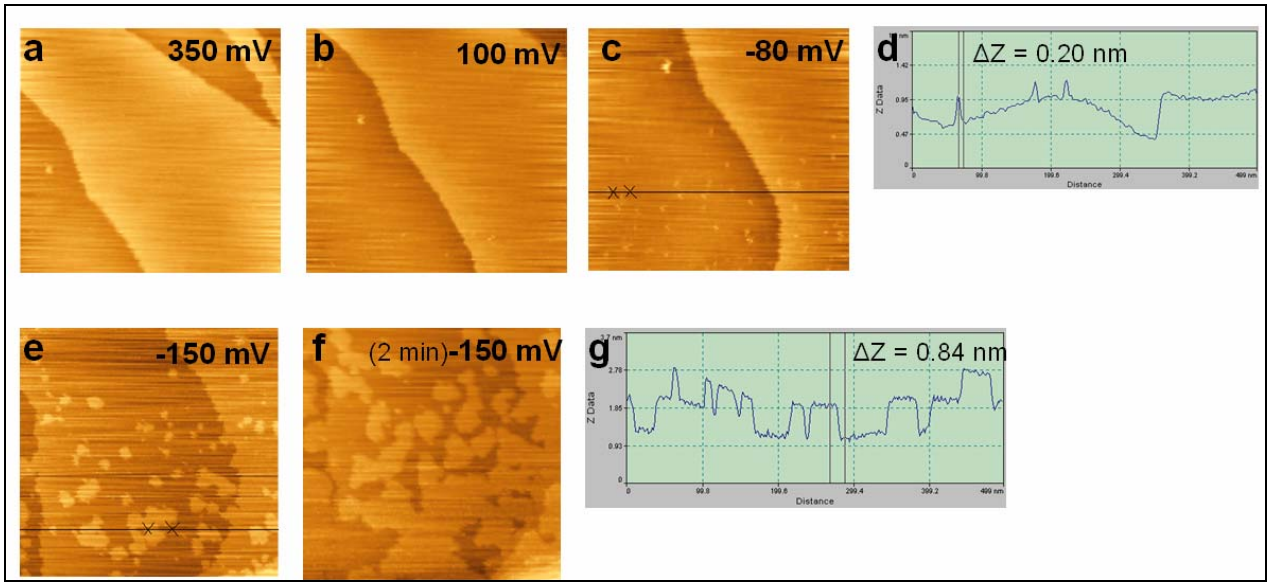

Figure 7.17: *In situ STM images (500 x 500 nm^2) of Au(111) in 1 mM thymine, 1 mM $AgClO_4$ + 0.1 M $HClO_4$, showing the UPD (a, b, c) and the OPD (e, f) processes. I_T = 1 nA, U_{bias} = -0.030 V. All potentials are refer to Ag/Ag^+ (0.1 M).* ***d*** *and* ***g*** *are the surface analysis of* ***c*** *and* ***e,*** *respectively.*

7.3 The Mechanism of Deposition of Silver on Thymine Modified Au(111)

As different from the Cu-UPD on thymine modified Au(111), where copper ions interact with physisorbed thymine prior to the UPD, during Ag-UPD silver ions interact with chemisorbed thymine molecules adsorbed on Au(111). To understand the action of adsorbed thymine on silver deposition processes one has to consider two steps during the layer formation:

(i) In a first step, silver ions have to penetrate the chemisorbed thymine layer and replace adsorbed thymine from the substrate. The replacement can take place as long as the adsorption of the silver ion is stronger than that of thymine. In case that the adsorption energy of the silver ion is equal or smaller than for thymine, the replacement cannot happen due to energetic reasons. It is hard to distinguish between the kinetic and energetic inhibition if the deposition process is completely suppressed on the time scale of the experiment. At this point, consideration of potentials of zero charge (PZC) change as a result of silver adlayer formation is an important step to understand the mechanism. For our experiment this means that PZC shifts to negative potentials (or increase of the positive surface charge) in the following order:

$$\text{Au(111)} \longrightarrow \text{AgML/Au(111)} \longrightarrow \text{Agbulk/Au(111)}$$

The adsorption strength between thymine and the respecting surface increases from Au(111) via the silver monolayer to the silver bulk substrates. Therefore, silver ions are able to push away thymine from the blank Au(111) surface.

(ii) In a second step, thymine molecules have to readsorb on the topmost metal layer. This readsorption may stabilize the metal layers which would support the deposition process. In case that the adsorption of thymine on the topmost layer is stronger than on the original substrate one has to expect an energy gain due to readsorption. Both effects, structure stabilization and adsorption energy gain support thermodynamically the deposition process. Consequently, the reduction potential shifts to more positive values. According to the increasing adsorption energy of thymine in the range

$$\text{Au(111)} \longrightarrow \text{AgML/Au(111)} \longrightarrow \text{Agbulk/Au(111)}$$

the readsorption of thymine on the topmost deposited metal layer leads for both the silver monolayer as well as the silver bulk to an energy gain.

Summarizing, it can be stated that the metal deposition on modified electrodes includes generally a combination of kinetic and energetic effects, which can act in same or in opposite directions. For our presented example of the deposition of silver on a thymine modified electrode this means that the first silver monolayer is formed in a reasonable time scale, whereas the deposition of the second monolayer is suppressed.

7.4 Summary

i) In pure $AgClO_4$ solution one ML of partially discharged silver is formed at higher underpotentials (0 V). Whereas, just positive of the Nernst potential (-0.120 V), 2 MLs of fully discharged silver is investigated. The second ML has most likely an expanded structure.

ii) In the presence of thymine, one ML of silver is deposited. Whereas, the formation of the 2^{nd} ML is almost blocked in the UPD region. Thymine is chemisorbed on the topmost silver layer via N(3).

iii) The 2^{nd} UPD and the OPD of silver are slightly hindered by the shielding effect of thymine molecules on top of silver monolayer. Upon OPD, thymine molecules are chemisorbed on the topmost partially discharged and expanded silver layer. The silver atoms below the topmost layer are fully discharged.

iv) The influence of chemisorbed thymine on silver deposition processes is strongly correlated to the energy balance between the adsorption energies of silver adatoms, thymine on the electrode and thymine on the final topmost layer.

v) Silver adatom adsorption obeys a Langmuir mechanism. It reveals obviously that the chemisorbed thymine molecules prevent the nucleation and growth mechanism.

vi) The EC-STM study performed in OPD region demonstrates a layer-by-layer growth (Frank-van der Merwe) rather than a three dimensional growth (Stranski-Krastanov) in the presence and absence of thymine.

vii) With time trace amounts of chloride ions present in the solution leads to the formation of insoluble AgCl at the surface.